ELSEVIER

PII: S0021-9290(96)00140-6

J. Biomechanics, Vol. 30, No. 6, pp. 539–548, 1997

Printed in Great Britain
0021-9290/97 $17.00 + .00

ESB Research Award 1996

BIOPHYSICAL STIMULI ON CELLS DURING TISSUE DIFFERENTIATION AT IMPLANT INTERFACES

P. J. Prendergast,*† R. Huiskes* and K. Søballe‡

*Biomechanics Section, Institute of Orthopaedics, University of Nijmegen, Nijmegen, The Netherlands; †Department of Mechanical Engineering, Trinity College, Dublin, Ireland; and ‡Department of Orthopaedics and Institute of Experimental Clinical Research, University Hospital of Århus, Denmark

Abstract—If musculoskeletal tissues are indeed efficient for their mechanical function, it is most reasonable to assume that this is achieved because the mechanical environment in the tissue influences cell differentiation and expression. Although mechanical stimuli can influence the transport of bioactive factors, cell deformation and cytoskeletal strain, the question of whether or not they have the potential to regulate tissue differentiation sequences (for example, during fracture healing or embryogenesis) has not been answered.

To assess the feasibility of biophysical stimuli as mediators of tissue differentiation, we analysed interfacial tissue formation adjacent to a micromotion device implanted into the condyles of dogs. A biphasic finite element model was used and the mechanical environment in the tissue was characterised in terms of (i) forces opposing implant motion, (ii) relative velocity between constituents, (iii) fluid pressure, (iv) deformation of the tissue and (v) strain in the tissue. It was predicted that, as tissue differentiation progressed, subtle but systematic mechanical changes occur on cells in the interfacial tissue. Specifically, as the forces opposing motion increase, the implant changes from being controlled by the maximum-allowable displacement (motion-control) to being controlled by the maximum-available load (force-control). This causes a decrease in the velocity of the fluid phase relative to the solid phase and a drop in interstitial fluid pressure accompanied by a reduction in peri-prosthetic tissue strains. The variation of biophysical stimuli within the tissue can be plotted as 'mechano-regulatory pathway', which identifies the transition from motion-control to force-control as a branching event in the tissue differentiation sequence. © 1997 Elsevier Science Ltd

Keywords: Tissue differentiation; Cell stimuli; Morphogenesis; Micromotion; Implant stability.

INTRODUCTION

It is an axiom of biomechanics that load-bearing tissues of the adult skeleton have reached a certain 'efficiency' with respect to their mechanical function (Carter *et al.*, 1996; Mow *et al.*, 1992). This could be achieved if the mechanical function generates appropriate patterns of biophysical stimuli in the tissue and if these biophysical stimuli could, in turn, be sensed by cells as part of a regulatory process. Cell sensitivity to biophysical stimuli has been studied intensively and mechanisms have been proposed—for example, biophysical stimuli alter cell shape which influences the cellular interaction with the biochemical environment (Stein and Bronner, 1989). It is presumed that the relationship between the mechanical forces on cells and biochemical environment generated by cell expressions, ultimately generates a harmonious relationship between the tissue and its mechanical function.

The events during the tissue formation processes of skeletal regeneration have been characterized (Pan and Einhorn, 1992) as (i) pooling of mesenchymal cells, (ii) mesenchymal cell differentiation and expression of collagen, (iii) calcification and angiogenesis accompanied by remodelling and (iv) osteoblast proliferation and bone formation. Wakitani *et al.* (1994) described chondral defect repair as a sequence starting with invasion of bioactive factors into the defect site, followed by differentiation of mesenchymal cells into chondrocytes. Collagen is then expressed interstitially to form a specialised collagenous network of water and ionised proteoglycan constituents. In both cases, the first event is the conglomeration of mesenchymal cells within the granulation tissue. The mesenchymal cells must then differentiate to form those cells which are capable of manufacturing the collagenous constituents of the intermediate and final load-bearing tissues. Fibrous connective tissues are generated by fibroblasts and cartilaginous tissues are generated by chondrocytes (Caplan, 1994). Cells committed to becoming osteoblasts and forming bone (osteoprogenitor cells) originate in the pluripotent cell pool of the stroma and they eventually lay down bony matrix (Owen, 1980).

Regarding the bone/implant interface, it is believed that the skeletal regeneration required for implant integration and stability is determined by micromotion at the bone/implant interface (Boyde and Jones, 1985; Weinans

Received in final form 5 *August* 1996. Presented in plenary session at the 10th Conference of the European Society of Biomechanics, Leuven, Belgium 28–31 August 1996.

Address correspondence to: Patrick J. Prendergast, Ph.D., University of Dublin, Department of Mechanical Engineering, Parsons Building, Trinity College, Dublin 2, Ireland.

et al., 1993). Sometimes a fibrous tissue layer develops, leading to loosening of the prosthesis, sometimes fibro-cartilage develops, and sometimes tissue differentiation occurs to form bone (Bechtold *et al.*, 1995; Rose *et al.*, 1984). Control of fibrous tissue differentiation at the bony implant bed is therefore important for implant/bone integration and long-term implant stability (Carter and Giori, 1991; Rubin and McLeod, 1994).

In pursuit of a further understanding of tissue differentiation, we calculated biophysical stimuli within regenerating tissues and attempted to relate the results with the survival of cells and the differentiation of new cell populations. We analysed an experiment previously reported by Søballe (1993a) by modelling the tissue as a biphasic material of both solid and fluid constituents (Mow *et al.*, 1980). We hypothesise that the mechanical environment is changed in a sufficiently systematic way that biophysical stimuli could stimulate the replacement of one cell population by another. If this is true then the regeneration of musculoskeletal tissues could be viewed as a tissue differentiation sequence that continues until a tissue type is formed which transfers appropriate biophysical stimuli, through the ECM, to the cells under functional loading.

METHODS

Review of the biological experiment

Søballe (1993a) reported an investigation of tissue regeneration during gap healing around a specially designed micromotion device implanted into the condyles of dogs (weight 21–35 kg), see Fig. 1.

Different tissues were found in the peri-implant gap as a function of (i) time after implantation, (ii) magnitude of micromotion, and (iii) implant-coating characteristics. Two levels of micromovement were used: 150 μm (Søballe *et al.*, 1992a) and 500 μm (Søballe *et al.*, 1992b). Two types of implant coating were used for each level of micromotion; plasma-sprayed titanium alloy implants and plasma-sprayed hydroxyapatite-coated implants. In Søballe *et al.* (1992a, b), all implants were subjected to micromotion for 4 weeks and the results were compared to stable controls. In a further study (Søballe *et al.*, 1993b), the 150 μm micromotion results were extended to 16 weeks, using two loading regimes: (i) 16 weeks of loading and (ii) four weeks of loading followed by 12 weeks of immobilisation by cutting the polyethylene plug.

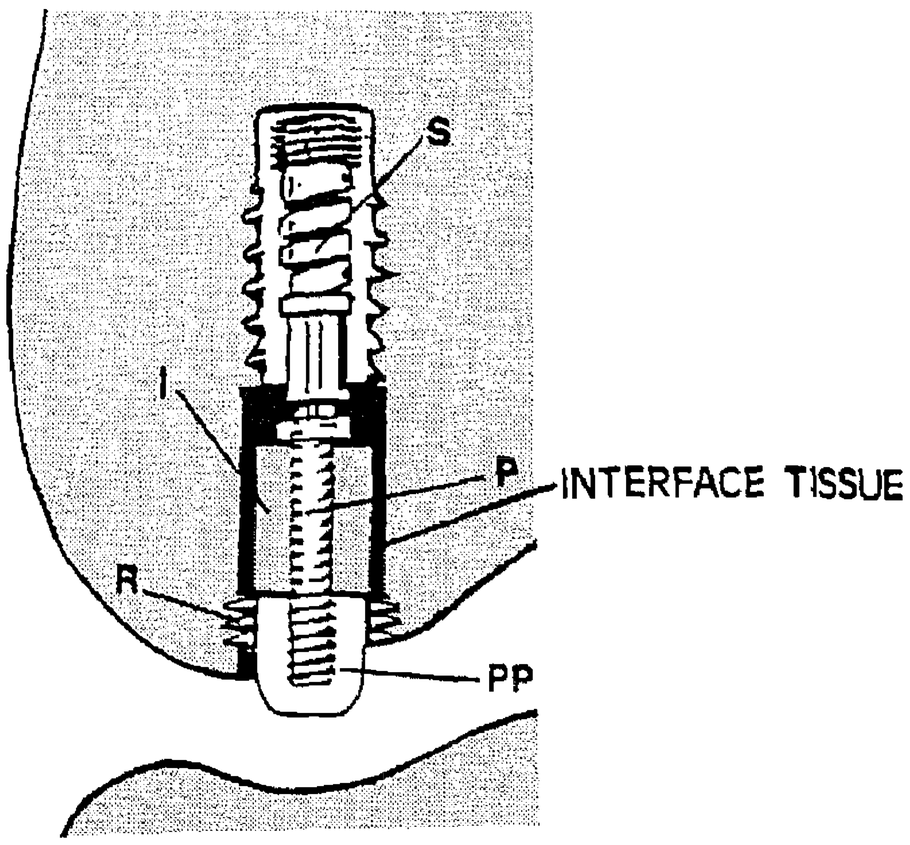

Fig. 1. A hollow screw is inserted into the condyle and stabilised by external threads. A piston (P) is mounted on a spring (S) and secured into the hollow screw. The distal part of the piston is threaded, and the implant (I) can be screwed onto it. The implant had a radius of 3 mm and was 10 mm long. The coating covers the implant, except for a 0.5 mm region at the proximal end. A polyethylene plug (PP) caps the piston and extends below the condyle surface. When the femur and tibia come together during the loading phase of gait, the implant is pushed into the bone; when the load is released the implant is returned to its distal position by the spring. A restraining collar limits the axial motion to either 150 or 500 μm (from Søballe *et al.*, 1993).

Push-out tests of the interfacial gap tissue were carried out for every experiment. Slices were cut of the implant/gap/bone system and placed on a rigid surface in which a 3.5 mm radius hole had been drilled. Given an implant radius of 3 mm, this meant that the implants were supported to within 500 μm of the tissue/implant interface. The implants were then preloaded to 2 N and held for approximately 10 s before application of a ramp displacement rate of 5 mm/min. The force/deflection curves were recorded. We have collected the data and plotted interfacial strength against time (Fig. 2). It is then easily seen that interfacial tissue growth is a process whose rate is retarded by greater micromotion and whose (initial) rate is increased by hydroxyapatite coating.

Interface tissues were also submitted to histological analysis. For the initial low strength phase, the tissue was described as predominantly 'fibrous connective tissue'; see Fig. 2. This included all the four-week experiments for the Ti-coated implants and only the 500 μm four-week experiment for the HA-coated implants. In the next phase, which is characterized by somewhat superior strength, the tissue included fibrocartilage. This included the four-week results for those HA implants which were stable and those subjected to the lower micromotion level of 150 μm, and the 16-week results for the 150 μm Ti implants. The third and the final phase was characterized by high strength. This included all the 16-week results, except the 16-week results for the 150 μm Ti-coated implants which are only in the second phase. The histological analysis showed that this final phase may be described as 'various amounts of bone' with some fibrocartilage.

From Jayes and Alexander (1978), it can be calculated that the maximum force generated at the canine knee is of the order of 300 N. Therefore, it is possible that, as the interfacial tissue stiffens, the implant will no longer displace the full amount of motion. Under such circumstances, *motion-control* would give way to *force-control*; a maximum load acts rather than a maximum displacement.

A mathematical description of the problem using the biphasic theory

Mow *et al.* (1980) present the biphasic theory as a development of the theory of mixtures. The principle of equipresence can be used to assert that each constituent of the mixture is present at each material point. Hence, a volume containing v constituents is given as

$$dV = dV^1 + dV^2 + \cdots + dV^v = \sum_{\alpha=1}^{v} dV^\alpha, \qquad (1)$$

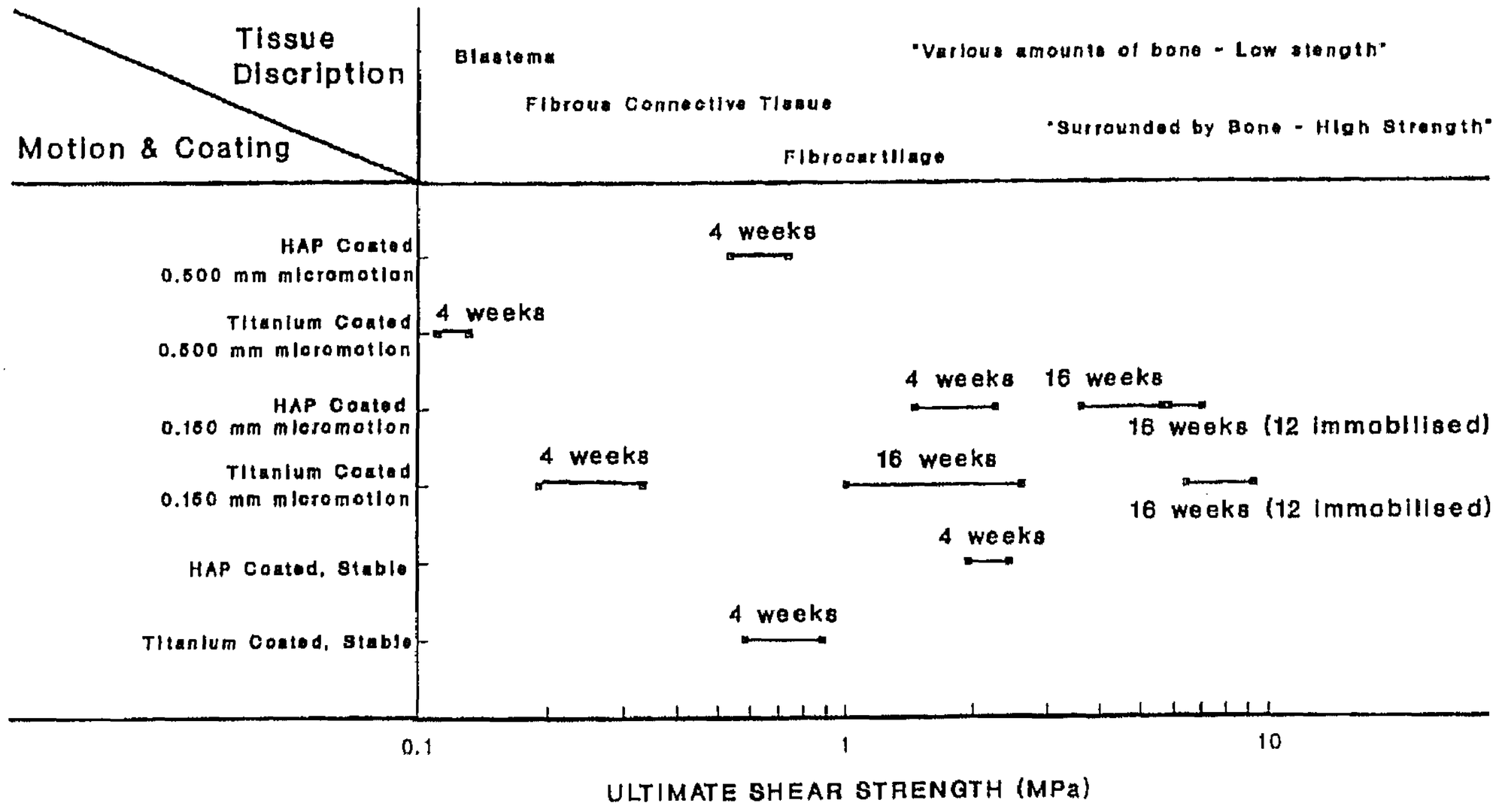

Fig. 2. Compendium of results from the push-out strength tests performed on interface gap tissue. The 150 μm, four-week results are from Table 2 of Søballe *et al.* (1992b). The 500 μm, four-week results are from Table 1 of Søballe *et al.* (1992a). The 150 μm, 16-week results are from Table 1 of Søballe *et al.* (1993). The results for the stable, four-week case can be taken from either Søballe *et al.* (1992b) where the controls were unloaded but stable or Søballe *et al.* (1992a) where the controls were loaded but stable. The former are plotted here. Note that the hydroxyapatite did not result in better mechanical strength of the interface after 16 weeks. We may assume from this result that the system is approaching a final tissue state at that stage. Note the log scale on the strength axis.

where α denotes the αth constituent. An apparent density ρ, and a true density ρ_T can be defined for each constituent as

$$\rho^\alpha = \frac{\mathrm{d}m^\alpha}{\mathrm{d}V}, \tag{2a}$$

$$\rho^\alpha_T = \frac{\mathrm{d}m^\alpha}{\mathrm{d}V^\alpha}, \tag{2b}$$

where $\mathrm{d}m^\alpha$ denotes mass of the αth constituent. The volume fraction of the αth constituent is given by $\phi^\alpha = \mathrm{d}V^\alpha/\mathrm{d}V$ and the particles of each constituent combine so as the apparent densities sum to the true density and the volume fractions sum to one. In a coordinate frame attached to the material point (material description) we write

$$\frac{\mathrm{D}}{\mathrm{D}T}(\rho^\alpha_T \mathrm{d}V^\alpha) = \frac{\mathrm{D}}{\mathrm{D}T}(\rho^\alpha_T \phi^\alpha \mathrm{d}V) = 0. \tag{3}$$

Note that the apparent density, ρ, changes, whereas, assuming incompressible constituents, the true density does not change, i.e. $\mathrm{D}\rho^\alpha_T/\mathrm{D}t = 0$. Describing the rate of volume change in terms of the local velocity components and converting to spatial coordinates, we get

$$\frac{\partial \phi^\alpha}{\partial t} + \nabla \cdot (\phi^\alpha \mathbf{v}^\alpha) = c^\alpha, \tag{4}$$

where ∇ is the gradient operator. Following Kelly (1964), the quantity c^α is included to describe the rate of supply of the αth constituent from all other constituents due to the reactive nature of the mixture. Cowin and Hegedus (1976) write a similar mass balance for the solid constituent only. The sum of the first and last terms of equation (4) is zero because, for the first term, if one constituent is displaced out of the differential volume, the space must be filled by another constituent, and for the second term, the reactions between constituents cannot create new matter. This gives the continuity equation for the mixture as

$$\sum_{\alpha=1}^{v} \nabla \cdot (\phi^\alpha \mathbf{v}^\alpha) = 0. \tag{5}$$

Conservation of linear momentum gives the equation of motion for the αth constituent as

$$\nabla \cdot \underline{\sigma} + \rho^\alpha \mathbf{q}^\alpha + \boldsymbol{\pi}^\alpha + \rho^\alpha_T c^\alpha \mathbf{v}^\alpha = \rho^\alpha \frac{\mathrm{D}\mathbf{v}^\alpha}{\mathrm{D}t}, \tag{6}$$

where $\underline{\sigma}^\alpha$ is the partial stress, $\mathbf{q}^\alpha$ is the body force per unit mass and $\boldsymbol{\pi}^\alpha$ is the rate of momentum supply to the αth constituent and $\rho^\alpha_T c^\alpha \mathbf{v}^\alpha$ is the momentum supply from biochemical reactions (Kelly, 1964). The internal forces resulting from such reactions can contribute to the partial stresses. This approach assumes that the particles coming into the αth constituent are kinematically indistinguishable from any pre-existing α constituent. The balance of linear momentum for the mixture as a whole requires that the sum of the momentum supplies is zero.

The constitutive relationships must satisfy thermodynamic constraints (i.e. the energy balance and the entropy inequality), as described by Mow *et al.* (1980). For a biphasic material in which the fluid is inviscid and each

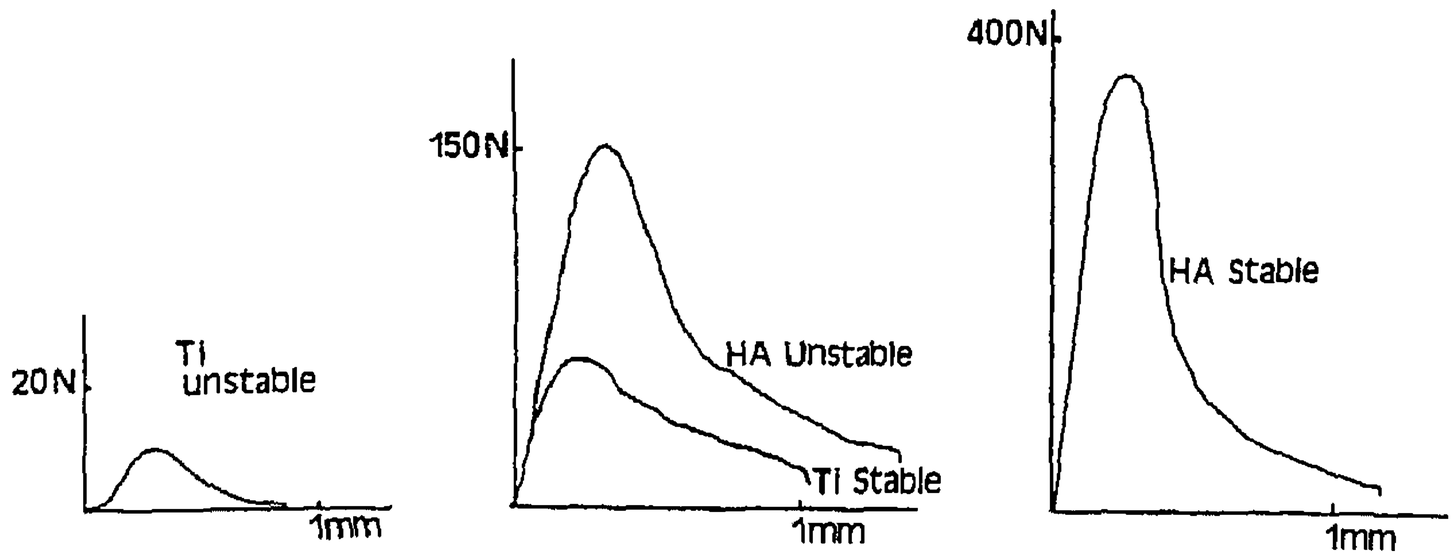

Fig. 3. Force/displacement curves recorded during push-out tests for stable titanium, unstable titanium, stable hydroxyapatite and unstable hydroxyapatite. The thickness of the push-out slice was different in each case, being equal to 2.69, 2.47, 2.62 and 2.75 mm, respectively.

constituent is isotropic, and where the infinitesimal strain–displacement relationship is assumed, we can write, following Mow *et al.* (1980);

$$\underline{\sigma}^{s} = \phi^{s} p I + \lambda^{s} e^{s} I + 2\mu^{s} \underline{\varepsilon}^{s}, \tag{7a}$$

$$\underline{\sigma}^{f} = -\phi^{f} p I. \tag{7b}$$

Where $\underline{\varepsilon}$ denotes strain and e denotes the dilatational strain. $(-)^{s}$ and $(-)^{f}$ denote solid-phase and fluid-phase quantities; p is the apparent pressure and λ^{s} and μ^{s} are the Lamé constants. Based on equation (7b) we could conclude that the divergence of the fluid stress is

$$\nabla \cdot \underline{\sigma}^{f} = -\nabla \phi^{f} p - \phi^{f} \nabla p. \tag{8}$$

The first term in equation (8), called the 'buoyancy force', is due to the resultant of the fluid pressure acting on the solid phase. For a medium with homogeneous porosity, this force is zero. Comparing with equation (6) and, given Darcy's law (Atkin and Craine, 1976), an expression for π^{s} in a mixture can be deduced as $\pi^{s} = K(\mathbf{v}^{f} - \mathbf{v}^{s})$. The momentum supply is due to the drag of the fluid phase against the solid phase at the fluid/solid interface. K is the diffusive drag coefficient and is related to permeability (Lai and Mow, 1980). To calculate the momentum supply from mass exchanges between the phases as a result of biochemical reactions we need an expression for one of either $c^{f}(t)$ or $c^{s}(t)$. In this study, the term was calculated using an equation of the form $c^{s}(t) = Ct^{n}$ where C and n are empirical constants.

Finite element model of peri-implant tissue

A finite element model was used to analyse the tissues, implemented using the soil mechanics capability of MARC (Palo Alto, U.S.A.); see Prendergast *et al.* (1996). The approach used eight-noded isoparametric elements which have pressure degrees-of-freedom at the corner nodes only. Thus, pressure is linearly interpolated within the element. The solution was iterated using a backward-Euler time-stepping scheme.

Push-out tests were used to determine Young's modulus of the interface tissues. Using axisymmetric finite element models for each push-out test, Young's modulus was estimated which gave the experimental force/deflection relationships for four different stages of interfacial fibrous tissue formation (see Fig. 3): Tissue 1—fibrous connective tissue, Tissue 2—inclusion of fibrocartilage, Tissue 3—fibrous tissue with small amounts of bone and Tissue 4—fibrous tissue with greater amounts of bone. A significant problem arises because the mechanical properties of the soft fibrous gap tissues have not been fully determined in mechanical tests. The permeability of the gap tissue had very little effect on the push-out analyses so it could not be identified. For the final analyses, estimates of permeability were made based on values reported for similar tissues (Armstrong and Mow, 1980; Levick, 1987) and from the fact that permeability decreases as solid fraction increases (Meijer, 1984; Simon, 1992). The cancellous bone was modelled as a biphasic material of Young's modulus equal to 4590 MPa (Choi *et al.*, 1990). The measured permeability for cancellous bone varies widely. Ochoa and Hillbery (1992) present 3.7×10^{-13} m^4/Ns as the average value in the proximal tibia and this value was used in the analyses.

An axisymmetric finite element mesh was used (Fig. 4). A prescribed axial displacement which increased to 150 μm in 0.5 s and reduced to zero in 0.5 s followed by 1 s at zero was applied to the implant/gap boundary. For force-control, motion continued until a maximum force of 300 N was obtained and held. The cancellous border was mechanically restrained and no fluid flow was permitted across the boundary. A zero pressure was prescribed at the distal gap.

The momentum transfer due to the reactivity of the gap tissue was expected to be small compared with the momentum transfer due to Stokes' drag. If it is assumed that a maximum solidity ϕ_{max} develops in a time T, then $C = (n+1)\phi_{max}/T$ (see the Appendix). Assuming, as a first approximation, that the solid-phase formation rate to be given by $n = 0$, and by using the observation of Søballe (1993a) that encapsulation by a fibrous phase ($\phi_{max} \cong 0.2$) was attained by four weeks, the reactivity term can be very roughly calculated and compared with the Stoke's drag term.

RESULTS

The Young's moduli of the interfacial tissues increased as tissue differentiation progressed; see Table 1. These results were obtained from the finite element models of the push-out tests.

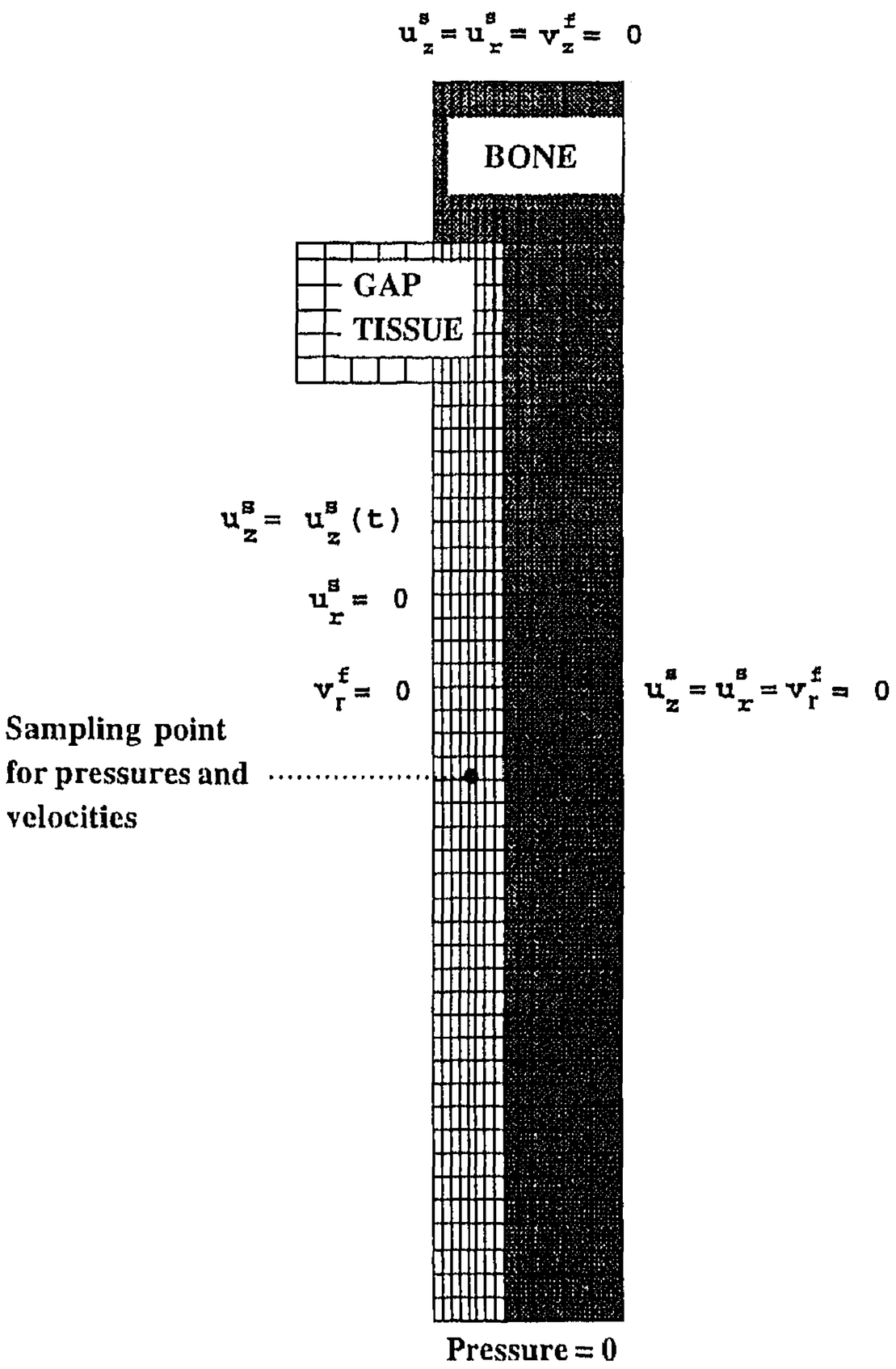

Fig. 4. The finite element model of the peri-implant gap tissue. In an attempt to model the effect that fluid flows into the bone, elements to represent cancellous bone 3 mm from the gap were included to allow fluid flow in the radial direction at the interface tissue/bone boundary. It was assumed that, at a certain distance into the cancellous bone, the effect due to the motion of the implant had become negligible.

Table 1. Young's moduli and permeability of the tissue used in the finite element analysis

	Young's modulus (MPa)	Permeability (m^4/N s)
Tissue 1	2	1×10^{-14}
Tissue 2	10	5×10^{-15}
Tissue 3	30	1×10^{-15}
Tissue 4	70	5×10^{-16}

Note: Compare Young's moduli of the following tissues:
(i) Bovine miniscal cartilage 0.410 ± 0.088 MPa (Proctor *et al.*, 1989).
(ii) Fibrous connective tissue 1.18–2.09 MPa at 0.45 MPa (Hori and Lewis, 1982).
(iii) Calcified cartilage 320 ± 250 MPa (Mente and Lewis, 1994).
(iv) Subchondral bone 1150 ± 370 MPa (Choi *et al.*, 1990).
(v) Trabecular bone tissue 4590 ± 160 MPa (Choi *et al.*, 1990).
Compare the permeability of the following tissues:
(i) Meniscal cartilage 1.26×10^{15} m^4/N s (Spilker *et al.*, 1992).
(ii) Human articular cartilage $4.7 \times 10^{-15} \pm 3.6 \times 10^{-15}$ m^4/N s (Armstrong and Mow, 1982).
(iii) Compact bone 1.0×10^{-17} m^4/N s (Johnson *et al.*, 1982).
(iv) Young canine tibial compact bone $3.53 \times 10^{-16} \pm 0.93 \times 10^{-16}$ m^4/N s (Li *et al.*, 1987).

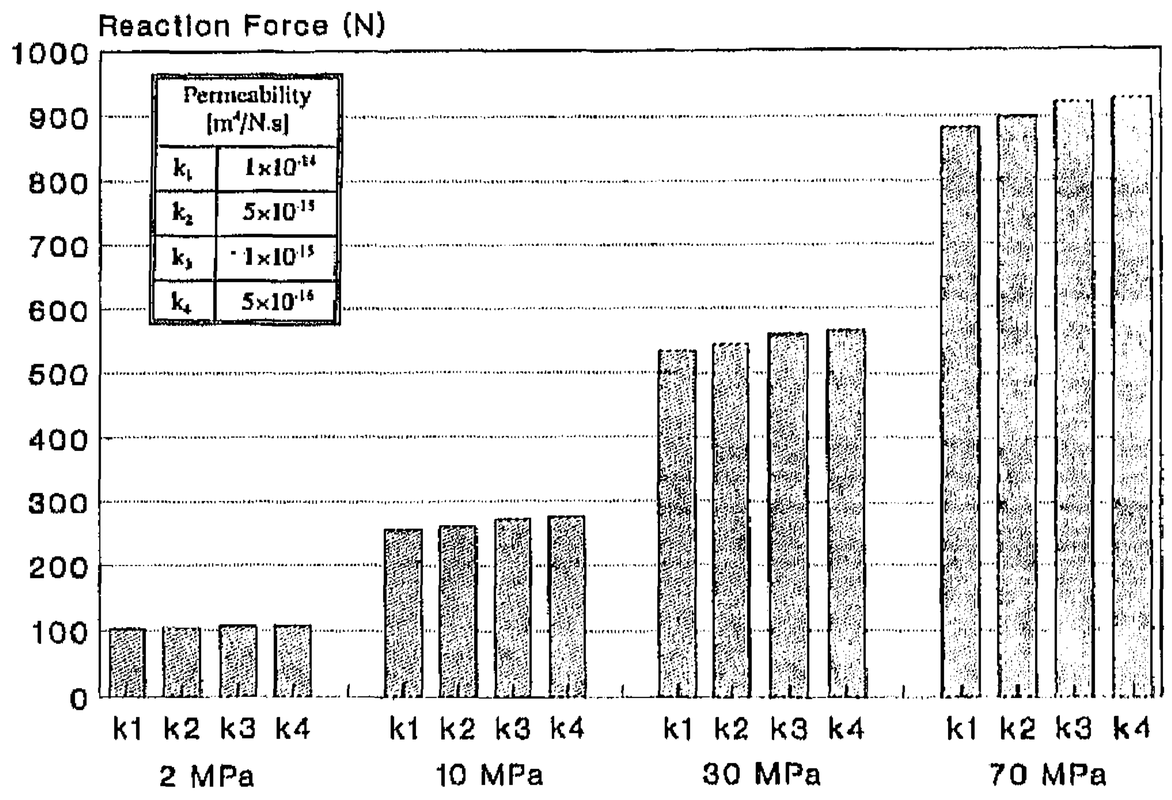

Fig. 5. The increase of reaction force (i.e. force opposing implant motion) during tissue regeneration for the four tissue states. For each Young's modulus, four different tissue permeabilities are analysed to show that the increase is independent of tissue permeability.

The reaction forces calculated at 150 μm micromotion show that the forces opposing implant micromotion increase during interfacial tissue regeneration; this result holds true for the full permutation of tissue properties given in Table 1 (see Fig. 5). The effect of decreasing the permeability is to further increase the reaction force, but only slightly. Given an estimated available force of 300 N at the knee of dogs, the calculations reported in Fig. 5 imply that the implant will no longer displace the full 150 μm for tissue states 3 and 4. The transition will be 'blurred' somewhat due to the randomness of the loading. Nevertheless, we can focus on two different loading types. The first is *motion-control* where a certain micromotion is maintained during tissue formation. The second is *force-control* where a certain maximum reaction force is carried whatever the displacement.

Peri-implant mechanical stimuli

As tissue regeneration proceeds, the maximum cyclic pressure was predicted to increase during *motion-control* and decrease during *force-control* (Fig. 6), whereas the velocity (Fig. 7) was predicted to decrease whether *motion-control* or *force-control* operated, though the decrease is larger under *force-control*. Hence, we can see that the mechanical effect of greater reaction force is paralleled by more subtle changes of the mechanical environment within the gap. Pressure and velocity were sampled at a position mid-way down the implant and half-way across the gap (Fig. 4), a similar position from where histological samples were taken by Søballe *et al.* (1992a, b; 1993) and Søballe (1993). Pressure and velocity did not vary substantially across the gap but there was a definite variation in the vertical direction indicating the importance of taking the histological samples from the same vertical position.

The need for a biphasic analysis is highlighted by the extent of the deflection of the interfacial tissue from a straight line (i.e. the linear elastic solution) which occurs because the micromotion device acts like a 'piston', forcing fluid to flow first outwards through the distal gap and then back in through the distal gap; see inset of Fig. 7.

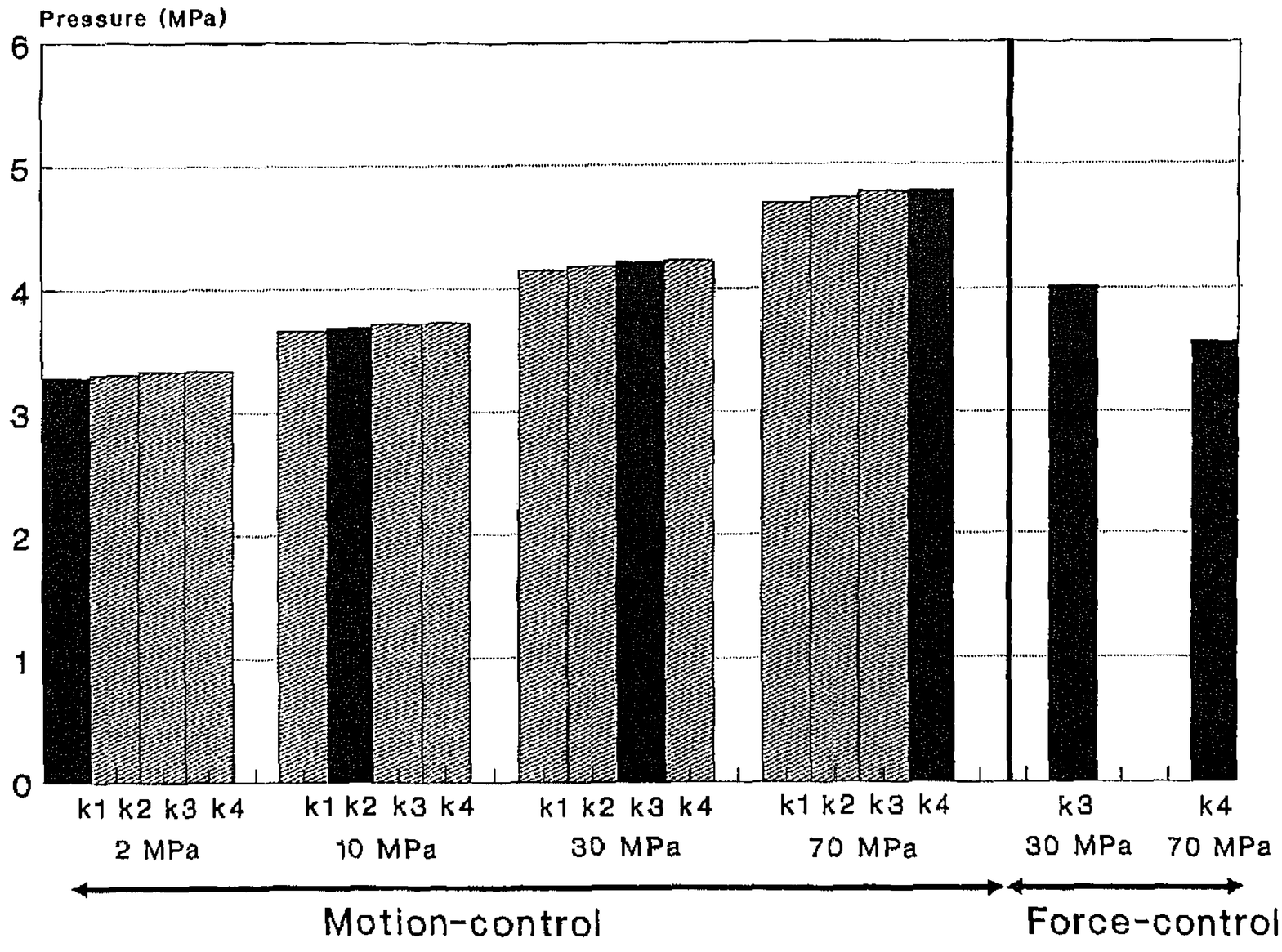

Fig. 6. The change of maximum cyclic pressure during tissue differentiation. The pressures generated when a full 150 μm was applied (*motion-control*) and when a maximum of 300 N was applied (*force-control*) are shown. The dark bars indicate the most likely combination of Young's modulus and permeability; see Table 1. The sampling position given in Fig. 5.

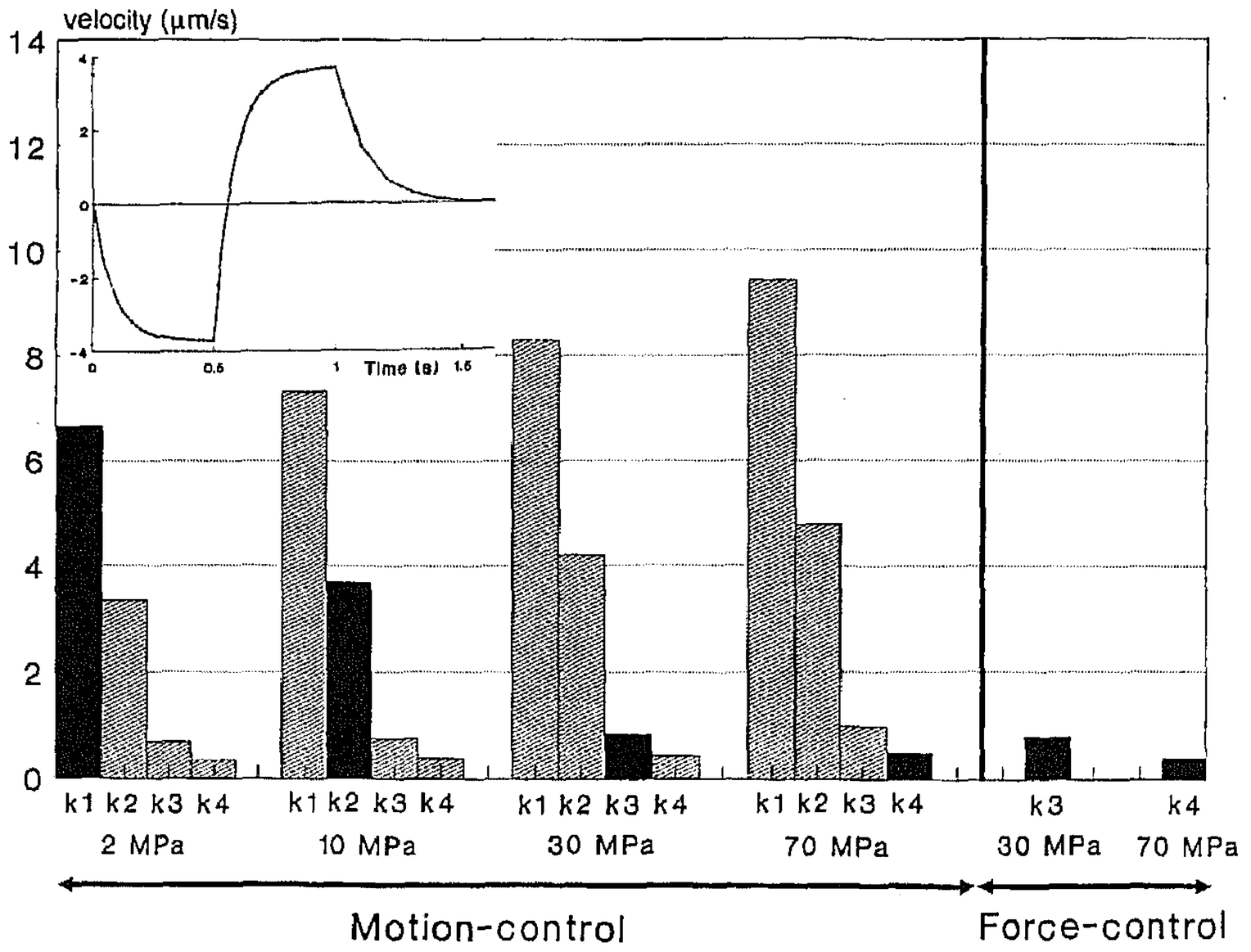

Fig. 7. The change of maximum cyclic velocity during tissue differentiation. The pressures generated when a full 150 μm was applied (*motion-control*) and when a maximum of 300 N was applied (*force-control*) are shown. The dark bars indicate the most likely combination of Young's modulus and permeability; see Table 1. The sampling position given in Fig. 5. The inset shows the cyclic velocity for Tissue 2 (i.e. with Young's modulus of 10 MPa and permeability of 5×10^{-15} m^4/Ns).

The result is a 'pumping' that generates a drag force in the tissue in the direction opposite to the motion of the implant. This effect is predicted to be dominant the early stages of tissue regeneration; see Fig. 8(a). As tissue differentiation progresses, the drag force is reduced relative to the forces generated by elastic stretching; see Fig. 9(a).

The Stokes' drag force has a substantial effect on the shear strain in the gap tissue in the initial stages of interfacial tissue regeneration; see Fig. 8(b). The effect is

differentiation—otherwise biophysical stimuli would be likely to have no regulatory influence.

The main limitation of the analysis is that the permeability of differentiating peri-prosthetic gap tissues is not known precisely. Since the parametric analysis has shown that the permeability has a dramatic influence on certain biophysical stimuli we must be cautious in interpreting the results. Armstrong and Mow (1982) determined that, as the equilibrium Young's modulus increases, the average permeability decreases. Similarly, Levick (1987) found that permeability decreases as collagen concentration increases. Based on these results, we may safely assume some decrease in permeability as Young's modulus increases during tissue differentiation, as in Table 1. It was predicted that the cyclic *pressure* increases with decreased tissue permeability, but that the effect did not overlap with the effect caused by Young's modulus. On the other hand, the predictions regarding fluid velocities are very dependent on permeability. However, since it is likely that the permeability reduces as tissue becomes stiffer, the prediction that relative velocity decreases during differentiation is most likely to hold true.

The effect of momentum change due to reactivity has been predicted to be small. However, the reason for this is that we did assume a linear tissue formation rate. It is worth noting that, in reality, tissue may form by locally rapid or 'explosive' reactions which would generate large local partial stresses which could have an influence on cell-level stimuli.

The mechanical stimuli in the gap can be summarized. In the beginning, the mechanical milieu is *motion-controlled*. The cyclic pressure is lowest, the relative velocity between the phases is highest and the shear strains near the implant and bone surfaces are high. This is the environment in which Søballe *et al.* (1992a, b; 1993) and Søballe (1993) find extensive presence of fibroblasts and later chondrocytes. The fibroblasts generate collagenous matrix and align it, causing stiffening of the solid phase and reducing the permeability (Levick, 1987). This causes a further fluid pressure increase and a further relative velocity decrease; the shear strain near the surface also decreases. In this environment, Søballe (1993) and Søballe *et al.* (1992a, b; 1993) find chondrocytes more so than fibroblasts. If *motion-control* were to persist, then it is likely that tissue development would reach a steady state at this stage. However, given the limited force available at the knee during gait, the predictions of the finite element model suggest that *force-control* will eventually arise at which time the implant will not bottom-out. If this is true, then the mechanical environment becomes one of even lower velocity between fluid and solid, decreased fluid pressure and, most significantly, lower shear strains. In this environment, Søballe *et al.* (1992a, b; 1993) and Søballe (1993) find eventual osteoblast proliferation.

The question to be answered is whether or not cells in the gap tissue are actually responding to the changed biophysical stimuli. The cell pool available for tissue regeneration consists of mesenchymal cells. Differentiation to fibroblasts is possible (Owen, 1980), and proliferation and migration of fibroblasts around the gap is the first cellular event reported by Søballe *et al.* (1992b). This leads to strengthening of the interfacial tissues in what we predict to be a high strain, high fluid velocity mechanical environment. Perhaps fibroblasts can maintain tractive contact with the collagen in this environment (Stopak and Harris, 1982). The next phase identified by Søballe *et al.* is the development of fibrocartilage in which chondrocytes are present. Chondrocytes can differentiate from the mesenchymal cell pool (Caplan, 1991). That this did not happen directly could be because mesenchymal cells will not differentiate into chondrocytes until a suitable mechanical environment is present. According to Caplan (1991)

> "the key factor in the conversion of a mesenchymal cell to a chondrocyte is maintaining the progenitor cell in a round, unspread confirmation".

This suggests that a reduction in the shearing (flow) of the fluid is needed—and this is indeed provided due to synthesis of collagen by fibroblasts and the attendant reduction of fluid velocity in the precursor cell pool. It fits with the evidence of these analyses that fibroblasts create a new mechanical environment (lower-flow, higher-pressure, lower-shear strain) in which they are no longer sustained. Furthermore, it is known that mechanical stimuli regulate chondrocyte cell metabolism and synthesis rates, and it is believed that chondrocytes have baroreceptors to sense the pressure (Stockwell, 1987). Therefore, the absence of a suited biophysical environment may be the reason why the chondrocyte cell population is not maintained. Rather osteoblast proliferation occurs and ossification proceeds. The present analysis predicts that pressure reduces as the tissue becomes stiffer when *force-control* loading is present. Reduced pressure is then accompanied by a substantial reduction in the relative velocity between the fluid and solid phases. Therefore, a reduction in fluid/solid velocity in the precursor cell pool, accompanied by a reduction in shear strain in the solid phase, would seem to be the circumstances favouring osteoblast proliferation, and hence interfacial ossification. It would therefore seem that cells synthesise an extracellular matrix in which a biophysical environment is set up which may or may not be suited to survival of that cell when competing against the other cell types capable of differentiating from the mesenchymal cell pool; see Weinans and Prendergast (1996) for a more general discussion of this point.

The hypothesised regulatory influence of mechanical factors on interfacial tissue development can be represented graphically as a mechano-regulatory pathway. Consider the mechanical environment to be represented by, say, two biophysical stimuli, the shear strain (x-axis) and cyclic fluid velocity (y-axis). The shear strain is a measure of the mechanical stimulus in the solid and the fluid velocity is a measure of the agitation in the precursor cell pool. As time progresses, cells will enter preprogrammed differentiation sequences and synthesize collagenous matrices. Collagen synthesis will automatically change the biophysical stimuli in the tissue. A trajectory of the time course of change of shear strain and cyclic fluid velocity can be drawn for any element in regenerating tissue as follows. At the start, the mechanical environment is one of the high surface shear strain and high fluid velocity. This is represented by a point on the $t = 0$ plane; see Fig. 10. Next, fibroblasts begin to

differentiation—otherwise biophysical stimuli would be likely to have no regulatory influence.

The main limitation of the analysis is that the permeability of differentiating peri-prosthetic gap tissues is not known precisely. Since the parametric analysis has shown that the permeability has a dramatic influence on certain biophysical stimuli we must be cautious in interpreting the results. Armstrong and Mow (1982) determined that, as the equilibrium Young's modulus increases, the average permeability decreases. Similarly, Levick (1987) found that permeability decreases as collagen concentration increases. Based on these results, we may safely assume some decrease in permeability as Young's modulus increases during tissue differentiation, as in Table 1. It was predicted that the cyclic *pressure* increases with decreased tissue permeability, but that the effect did not overlap with the effect caused by Young's modulus. On the other hand, the predictions regarding fluid velocities are very dependent on permeability. However, since it is likely that the permeability reduces as tissue becomes stiffer, the prediction that relative velocity decreases during differentiation is most likely to hold true.

The effect of momentum change due to reactivity has been predicted to be small. However, the reason for this is that we did assume a linear tissue formation rate. It is worth noting that, in reality, tissue may form by locally rapid or 'explosive' reactions which would generate large local partial stresses which could have an influence on cell-level stimuli.

The mechanical stimuli in the gap can be summarized. In the beginning, the mechanical milieu is *motion-control*. The cyclic pressure is lowest, the relative velocity between the phases is highest and the shear strains near the implant and bone surfaces are high. This is the environment in which Søballe *et al.* (1992a, b; 1993) and Søballe (1993) find extensive presence of fibroblasts and later chondrocytes. The fibroblasts generate collagenous matrix and align it, causing stiffening of the solid phase and reducing the permeability (Levick, 1987). This causes a further fluid pressure increase and a further relative velocity decrease; the shear strain near the surface also decreases. In this environment, Søballe (1993) and Søballe *et al.* (1992a, b; 1993) find chondrocytes more so than fibroblasts. If *motion-control* were to persist, then it is likely that tissue development would reach a steady state at this stage. However, given the limited force available at the knee during gait, the predictions of the finite element model suggest that *force-control* will eventually arise at which time the implant will not bottom-out. If this is true, then the mechanical environment becomes one of even lower velocity between fluid and solid, decreased fluid pressure and, most significantly, lower shear strains. In this environment, Søballe *et al.* (1992a, b; 1993) and Søballe (1993) find eventual osteoblast proliferation.

The question to be answered is whether or not cells in the gap tissue are actually responding to the changed biophysical stimuli. The cell pool available for tissue regeneration consists of mesenchymal cells. Differentiation to fibroblasts is possible (Owen, 1980), and proliferation and migration of fibroblasts around the gap is the first cellular event reported by Søballe *et al.* (1992b). This leads to strengthening of the interfacial tissues in what we predict to be a high strain, high fluid velocity mechanical environment. Perhaps fibroblasts can maintain tractive contact with the collagen in this environment (Stopak and Harris, 1982). The next phase identified by Søballe *et al.* is the development of fibrocartilage in which chondrocytes are present. Chondrocytes can differentiate from the mesenchymal cell pool (Caplan, 1991). That this did not happen directly could be because mesenchymal cells will not differentiate into chondrocytes until a suitable mechanical environment is present. According to Caplan (1991)

> "the key factor in the conversion of a mesenchymal cell to a chondrocyte is maintaining the progenitor cell in a round, unspread confirmation".

This suggests that a reduction in the shearing (flow) of the fluid is needed—and this is indeed provided due to synthesis of collagen by fibroblasts and the attendant reduction of fluid velocity in the precursor cell pool. It fits with the evidence of these analyses that fibroblasts create a new mechanical environment (lower-flow, higher-pressure, lower-shear strain) in which they are no longer sustained. Furthermore, it is known that mechanical stimuli regulate chondrocyte cell metabolism and synthesis rates, and it is believed that chondrocytes have baroreceptors to sense the pressure (Stockwell, 1987). Therefore, the absence of a suited biophysical environment may be the reason why the chondrocyte cell population is not maintained. Rather osteoblast proliferation occurs and ossification proceeds. The present analysis predicts that pressure reduces as the tissue becomes stiffer when *force-control* loading is present. Reduced pressure is then accompanied by a substantial reduction in the relative velocity between the fluid and solid phases. Therefore, a reduction in fluid/solid velocity in the precursor cell pool, accompanied by a reduction in shear strain in the solid phase, would seem to be the circumstances favouring osteoblast proliferation, and hence interfacial ossification. It would therefore seem that cells synthesise an extracellular matrix in which a biophysical environment is set up which may or may not be suited to survival of that cell when competing against the other cell types capable of differentiating from the mesenchymal cell pool; see Weinans and Prendergast (1996) for a more general discussion of this point.

The hypothesised regulatory influence of mechanical factors on interfacial tissue development can be represented graphically as a mechano-regulatory pathway. Consider the mechanical environment to be represented by, say, two biophysical stimuli, the shear strain (x-axis) and cyclic fluid velocity (y-axis). The shear strain is a measure of the mechanical stimulus in the solid and the fluid velocity is a measure of the agitation in the precursor cell pool. As time progresses, cells will enter preprogrammed differentiation sequences and synthesize collagenous matrices. Collagen synthesis will automatically change the biophysical stimuli in the tissue. A trajectory of the time course of change of shear strain and cyclic fluid velocity can be drawn for any element in regenerating tissue as follows. At the start, the mechanical environment is one of the high surface shear strain and high fluid velocity. This is represented by a point on the $t = 0$ plane; see Fig. 10. Next, fibroblasts begin to

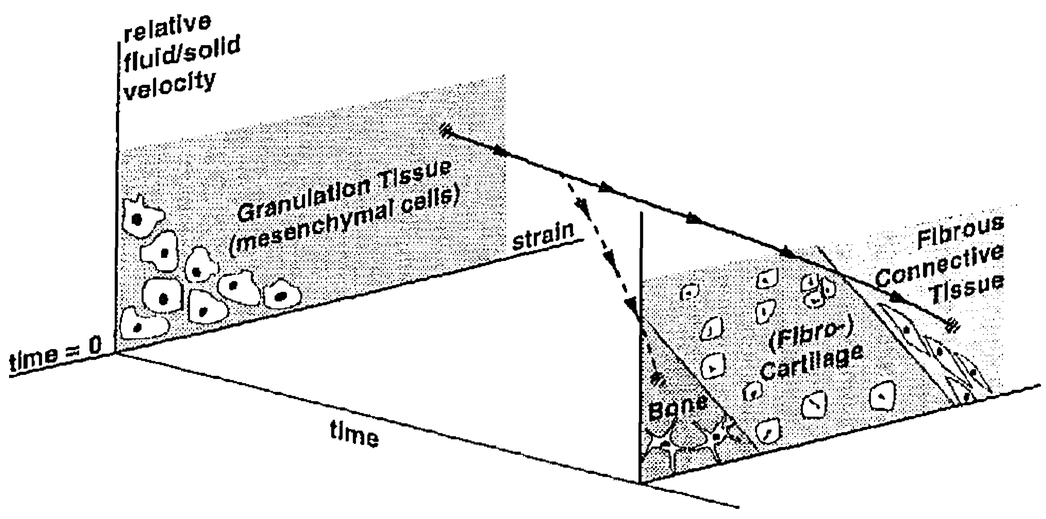

Fig. 10. A 'mechano-regulatory pathway' can be used to describe the hypothesised interaction between biophysical stimuli and tissue phenotype. In this case, two biophysical stimuli are used (i) the shear strain in the solid phase and (ii) the relative velocity between the fluid and the solid. The mechano-regulatory pathway is then a curve in R^3. Certain collagenous matrices are synthesised by the cells in the tissue, as a function of time. If the situation is such that a certain motion is maintained (*motion-control* given by the full line) then the shear strain stays high and no bone will form. On the other hand, if the synthesis of more collagen can cause the motion to reduce (*force-control* given by the dashed line) then the shear strains and relative velocities will reduce and ossification will occur—but intermediate tissue types (tissue differentiation) may be required.

express collagen which increases the tissue's Young's modulus and decreases its permeability. The mechanical environment changes to reduced fluid velocity and reduced shear strain, describing a trajectory as shown. At some stage the implant no longer 'bottoms out', at which time *motion-control* gives way to *force-control*. The dashed line indicates the trajectory of *force-control* predicted by the results of the finite element analyses. The *force-control* situation causes a greater reduction in the fluid velocity and a reduction in the shear strain in the tissue, towards a target of low shear strain and low fluid velocity when ossification occurs.

In conclusion, systematic changes in biophysical stimuli are predicted to occur in peri-implant regenerating tissue. This suggests that there may be boundaries between mechanical states in the tissue such that, when the boundary is crossed, cell-driven biochemical reactions are initiated which switch the tissue from one type to another by tissue differentiation. Therefore, the results support the hypothesis that the mechanical environment in the tissue has a controlling influence on tissue differentiation. To prove the generality of this proposition, similar mechanical stimuli changes would need to be found in other differentiating systems, such as during fracture healing or embryogenesis.

Acknowledgements—This work was funded by a grant 'The Structural Modelling of Bone/Implant Interfaces' form the European Commission—Directorate-General for Science, Research and Development. It is a pleasure to thank Willem Dirk van Driel, M.S., for his contribution to this research. Dr M. C. H. van der Meulen and Dr H. Weinans are thanked for general discussions and inputs to Fig. 10. Dr E. S. Hansen, Dr H. Brokstedt and Prof. C. Bünger are thanked for assistance during the experimental phase.

REFERENCES

Armstrong, C. G. and Mow, V. C. (1982) Variations in the intrinsic mechanical properties of human articular cartilage with age, degeneration and water content. *J. Bone Jt Surg.* **64A**, 88–94.

Atkin, R. J. and Craine, R. E. (1976) Continuum theories of mixtures: applications. *J. Inst. Maths Applics* **17**, 153–207.

Bechtold, J. E., Søballe, K., Lewis, J. L. and Gustilo, R. B. (1995) The roles of implant motion and particulate debris in the formation of an agressive prerprosthetic membrane. *Trans. 41st Orthop. Res. Soc.* p. 767.

Boyde, A. and Jones, S. J. (1985) Bone modelling in the implantation bed. *J. Biomed. Mater. Res.* **19**, 199–224.

Caplan, A. I. (1991) Mesenchymal stem cells. *J. Orthop. Res.* **9**, 641–650.

Caplan, A. I. (1994) The mesengenic process. *Clin. Plast. Surg.* **21**, 429–435.

Carter, D. R. and Giori, N. J. (1991) Effect of mechanical stress on tissue differentiation in the bony implant bed. In *The Bone–Biomaterial Interface*, ed. J. E. Davies, pp. 367–376. University of Toronto Press, Toronto.

Carter, D. R., van der Meulen, M. C. H. and Beaupré, G. S. (1996) Mechanical factors in bone growth and development. *Bone* **18**, 5S–10S.

Choi, K., Kuhn, J. L., Ciarelli, M. J. and Goldstein, S. A. (1990) The elastic moduli of human subchondral, trabecular and cortical bone tissue and the size-dependency of cortical bone modulus. *J. Biomechanics* **23**, 1103–1113.

Cowin, S. C. and Hegedus, D. H. (1976) Bone remodelling I: theory of adaptive elasticity. *J. Elasticity* **6**, 313–326.

Hori, R. Y. and Lewis, J. L. (1982) Mechanical properties of the fibrous tissue found at the bone-cement interface following total joint replacement. *J. Biomed. Mater. Res.* **16**, 911–927.

Jayes, A. S. and Alexander, R. McN. (1978) Mechanics of locomotion of dogs (Canis familiaris) and sheep (Ovis aries). *J. Zool., Lond.* **185**, 289–308.

Johnson, M. W., Chakkalakal, D. A., Harper, R. A., Katz, J. L. and Rouhana, S. W. (1982) Fluid flow in bone *in vitro*. *J. Biomechanics* **15**, 881–885.

Kelly, P. D. (1964) A reacting continuum. *Int. J. Engng Sci.* **2**, 129–153.

Lai, W. M. and Mow, V. C. (1980) Drag-induced compression of articular cartilage during a permeation experiment. *Biorheology* **17**, 111–123.

Levick, J. R. (1987) Review article: flow through interstitium and other fibrous matrices. *Q. J. Exp. Physiol.* **72**, 409–438.

Li, G., Bronk, J. T., An, K.-N. and Kelly, P. J. (1987) Permeability of cortical bone of canine tibiae. *Microvascular Res.* **34**, 302–310.

Meijer, K. L. (1984) Comparison of finite and infinitisimal strain consolidation by numerical experiments. *Int. J. Numer. Methods Geomech.* **8**, 531–548.

Mente, P. L. and Lewis, J. L. (1994) Elastic modulus of calcified cartilage is an order of magnitude less than that of subchondral bone. *J. Orthop. Res.* **12**, 637–647.

Mow, V. C., Kuei, S. C., Lai, W. M. and Armstrong, C. G. (1980) Biphasic creep and stress relaxation of articular cartilage: theory and experiments. *J. Biomech. Engng* **102**, 73–84.

Mow, V. C., Ratcliffe, A. and Poole, A. R. (1992) Cartilage and diathrodial joints as paradigms for hierarchical materials and structures. *Biomaterials* **13**, 67–97.

Ochoa, J. A. and Hillberry, B. M. (1992) Permeability of bovine cancellous bone. *Trans. 38th Orthop. Res. Soc.* p. 162.

Owen, M. (1980) The origin of bone cells in the postnatal organism. *Arth. Rheum.* **23**, 1073–1079.

Pan, W. T. and Einhorn, T. A. (1992) The biochemistry of fracture healing. *Curr. Orthop.* **6**, 207–213.

Pauwels, F. (1941) Grundriß einer Biomechanik der Frakturheilung. In *34th Kongress der Deutschen Orthopädischen Gesellschaft*, pp. 62–108. Ferdinand Enke Verlag, Stuttgart.

Pauwels, F. (1980) A new theory concerning the influence of mechanical stimuli on the differentiation of the supporting tissues. In *Biomechanics of the Locomotor Apparatus* (Translated from the 1965 German Edition by P. Manquet and R. Furlong), pp. 375–407. Springer, Berlin.

Prendergast, P. J., van Driel, W. D. and Kuiper, J.-H. (1996) A comparison of finite element codes for the solution of biphasic poroelastic problems. *Proc. Instn Mech. Engrs* **210**, 131–136.

Proctor, C. S., Schmidt, M. B., Whipple, R. R., Kelly, M. A. and Mow, V. C. (1989) Material properties of the normal bovine medial meniscus. *J. Orthop. Res.* **7**, 771–782.

Rose, R. M., Martin, R. B., Orr, R. B. and Radin, E. L. (1984) Architectural changes in the proximal femur following prosthetic insertion:

preliminary observations on an animal model. *J. Biomechanics* **17,** 241–249.
Roux, W. (1912) Anpassungslehre, Histomechanik und Histochemie. Mit Bemerkungen über die Entwicklung und Formgestaltung der Gelenke (Adaptation, histomechanics and histochemistry, with a notation concerning development and formation of bones). *Virchows Arch. Pathologische Anatomie Physiologie Klinische Medizin (Berlin)* **209,** 168–209.
Rubin, C. T. and McLeod, K. J. (1994) Promotion of bony ingrowth by frequency-specific, low-amplitude mechanical strain. *Clin. Orthop.* **298,** 165–174.
Simon, B. R. (1992) Multiphase poroelastic finite element models for soft tissue structures. *Appl. Mech. Rev.* **45,** 191–218.
Søballe, K. (1993) Hydroxyapatite ceramic coating for bone implant fixation. Mechanical and histological studies in dogs. *Acta Orthop. Scand.* **64** (*Suppl.* 255).
Søballe, K., Hansen, E. S., B-Rasmussen, H., Jørgensen, P. H. and Bünger, C. (1992a) Tissue ingrowth into titanium and hydroxyapatite coated implants during stable and unstable mechanical conditions. *J. Orthop. Res.* **10,** 285–299.
Søballe, K., B-Rasmussen, H., Hansen, E. S. and Bünger, C. (1992b) Hydroxyapatite coating modifies implant membrane formation. Controlled micromotion studied in dogs. *Acta Orthop. Scand.* **63,** 128–140.
Søballe, K., Hansen, E. S., B-Rasmussen, H. and Bünger, C. (1993) Hydroxyapatite coating converts fibrous tissue to bone around loaded implants. *J. Bone Jt Surg.* **75B,** 270–278.
Spilker, R. L., Donzelli, P. S. and Mow, V. C. (1992) A transversely isotropic biphasic finite element model of the meniscus. *J. Biomechanics* **25,** 1027–1045.
Stein, W. D. and Bronner, F. (1989) (eds) *Cell Shape. Determinants, Regulation and Regulatory Role.* Academic Press, Inc., San Diego.
Stockwell, R. A. (1987) Structure and function of the chondrocyte under mechanical stress. In *Joint Loading: Biology and Health of Articular Structures*, eds H. Helminen, I. Kiviranta, A.-M. Säämänen, M. Tammi, K. Paukkonen and J. Jurvelin, pp. 126–148. John Wright, Bristol.
Stopak, D. and Harris, A. K. (1982) Connective tissue morphogenesis by fibroblast traction. 1. Tissue culture observations. *Dev. Biol.* **90,** 383–398.
Wakitani, S., Goto, T., Pineda, S. J., Young, R. G., Mansour, J. M., Caplan, A. I. and Goldberg, V. M. (1994) Mesenchymal cell-based repair of large, full-thickness defects of articular cartilage. *J. Bone Jt Surg.* **76A,** 579–592.
Weinans, H., Huiskes, R. and Grootenboer, H. J. (1993) Quantative analysis of bone reactions to relative motions at implant-bone interfaces. *J. Biomechanics* **26,** 1271–1281.
Weinans, H. and Prendergast, P. J. (1996) Tissue adaptation as a dynamical process far from equilibrium. *Bone* **19,** 143–149.

APPENDIX

c^α is the rate of supply of the solid constituent, i.e.

$$\frac{d\phi^s}{dt} = c^s$$

substituting

$$\phi^s = \int_0^t Ct^n \, dt = \frac{Ct^{n+1}}{(n+1)}.$$

At time T, $\phi^s = \phi^s_{max}$; therefore

$$C = \frac{\phi^s_{max}(n+1)}{T^{n+1}}.$$